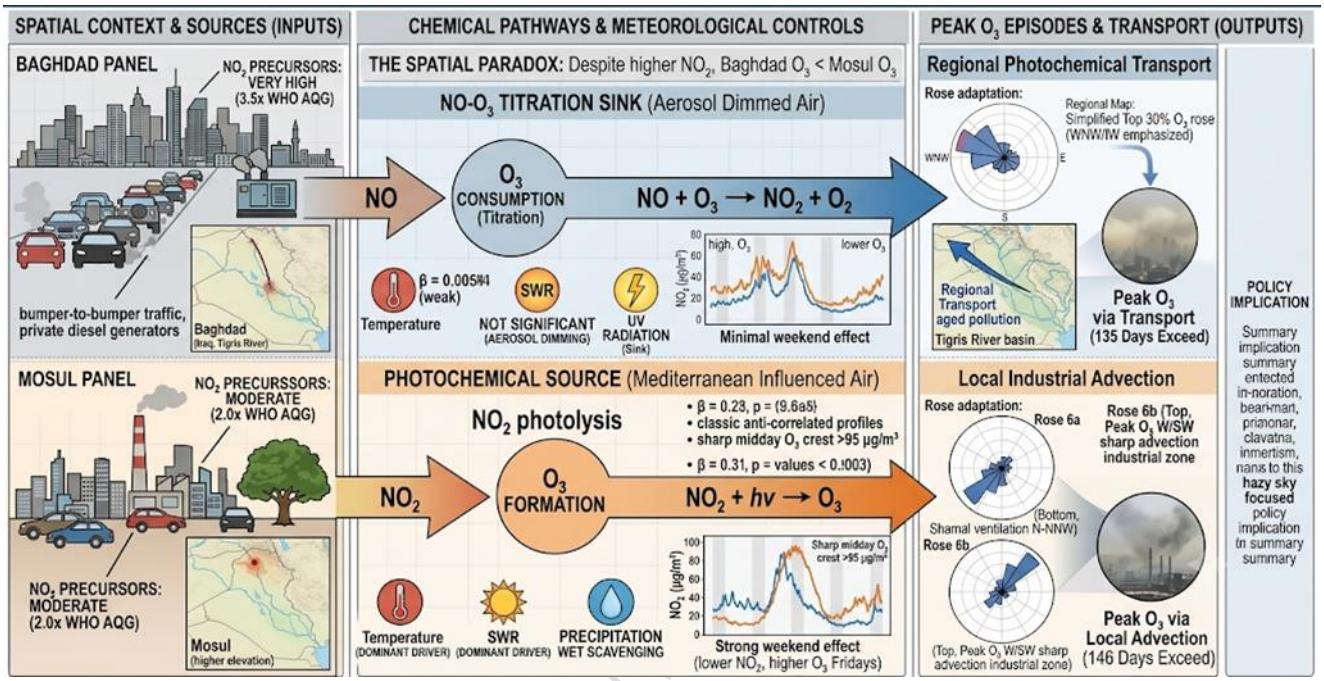
Effect of city site, size, and some meteorological factors on NO_2 and O_3 concentrations

Abdulmuhsin S. Shihab[1]*, Musab A. Altamir[1], Ammar Th. Hamad[1]

[1] Environmental Engineering Department, College of Engineering, University of Mosul, Mosul, Iraq

* Corresponding Author's e-mail: mss_qzz@uomosul.edu.iq

Graphical abstract



Abstract

The study tries to compare the spatiotemporal characteristics of NO_2 and O_3 in Baghdad and Mosul using 2022 monitoring data to find the influence of meteorological factors. Baghdad showed substantially higher annual NO_2 concentrations (36.7 µg/m³) than Mosul (21.2 µg/m³), with exceedance days 129 in Mosul and 285 in Baghdad, while Mosul shows higher annual O_3 levels (58.1 µg/m^3) than Baghdad (53.1 µg/m^3) caused weaker NO-titration. Both cities repeatedly exceeded the WHO 8-hour O_3 guideline, 146 days for Mosul and 135 days for Baghdad. Besides, the highest peak season concentration of O_3 exceeded the WHO guidelines and reached 111.8 µg/m^3 in Mosul and 108.8 µg/m^3 in Baghdad. Temperature was the dominant driver of O_3, while atmospheric pressure supported NO_2 accumulation and wind speed improved pollutant dispersion. Shortwave radiation greatly influenced O_3 formation in Mosul, while UV radiation played a more role in Baghdad because of aerosol dimming. Pollution rose analysis found that peak O_3 in Mosul was mainly related with local industrial emissions, while in Baghdad it was related to regional photochemical transport. These findings emphasize the importance of city-specific air quality management strategies.

Keywords: Air quality, Baghdad, Meteorological factors, Mosul, NO_2, O_3

ACCEPTED

1. Introduction

The strategies of countries to control emissions always include nitrogen dioxide (NO_2) and ozone (O_3) monitoring due to their adverse impacts on human health and ecosystems especially in urban areas (Yin *et al.*, 2017; Xia *et al.*, 2024). Recent studies found that the exposure to NO_2 and O_3 may increase the risk of respiratory and cardiovascular diseases (Tao *et al.*, 2012; Huangfu and Itkinson, 2020; Abdipour et al., 2025; Abdipour et al., 2026). Furthermore, it may cause irritation to eye and skin (Choi *et al.*, 2024; Han *et al.*, 2025).

NO_2 is a primary pollutant produced from fuel combustion in vehicles, while O_3 is a secondary pollutant produced by complex photochemical reactions including nitrogen oxides and volatile organic compounds in sunlight. Due to the chemical relating of ozone and nitrogen oxides, the levels of NO_2 and O_3 are inseparably linked. Therefore, any decrease in the level of NO_2 is associated with an increase in O_3 levels (Han *et al.*, 2011).

The levels of NO_2 and O_3 in the atmosphere are affected not only by emission sources, but also by environmental and urban factors like geographical location, topography and size of the city. Additionally, many researches had shown the effect of meteorological factors such as temperature, wind speed and solar radiation on dispersion and formation of NO_2 and O_3 (Kobza *et al.*, 2024; Chen and Dai, 2024; Chatoutsidou *et al.*, 2026).

Iraq's large cities encounter expanding air quality challenges forced by rapid urbanization, increasing vehicle fleets, industrial emissions and diesel generators during power cease. In spite of that, there are a limited number of studies analyzing NO_2 and O_3 levels in Iraq and its relationships with meteorological parameters. Additionally, there is a weak knowledge gap regarding the simultaneous comparative assessment of NO_2 patterns and tropospheric 8-hour average O_3 dynamic across contrasting urban topographic and emission profiles in Iraq (specially Baghdad vs. Mosul). These limited studies depend on interrupted ground-based data or on satellite data. Shihab and Al-Jarrah (2015) studied the levels of O_3 and nitrogen oxides in Mosul city. For that reason, the monitoring and the analysis of pollutants are essential to prepare efficient programs for decreasing pollution and save human health. In addition, comparative studies among cities with different urban profiles are required to find the pollution dynamics. This work fills this gap by using high-resolution spatiotemporal monitoring data to explain the photochemical coupling of NO_2 and O_3, presenting an integrated basis for urban air quality management.

The study aims to investigate the effect of city characteristics (site and size) and selected meteorological variables on NO_2 and O_3 concentration. The outcomes may help planning policies directed to reduce pollution exposure.

ACCEPTED MANUSCRIPT

2. Materials and methods

2.1 Site description

Two main cities in Iraq were chosen to study the impact of size and site on NO_2 and O_3 levels; Baghdad (the capital of Iraq) and Mosul, the second largest city after Baghdad, as shown in **Figure 1**. Baghdad in the middle of Iraq located along the Tigris River, with an elevation of around 34 meters above sea level with an area of 700 square kilometers (metropolitan area), and an estimated population of about 8 million (roughly 12,000 per square kilometer). On the other hand, Mosul is located about 450 km north of Baghdad and is sited on the Tigris River, at an elevation of 223 meters above sea level, overlaying about 180 square kilometers with a population of about 1.90 million (about 10,000 per square kilometer) (Alnajm, 2023; Encyclopedia Britannica, 2025; Iraq-Wikipedia, n.d.; Ministry of Planning, n.d.). Baghdad's terrain is mainly flat with an arid climate, while Mosul is located closer to the foothills of the Zagros Mountains, resulting in slightly more diverse terrain, cooler temperatures, and slightly higher precipitation levels (Jassim & Goff, 2006).

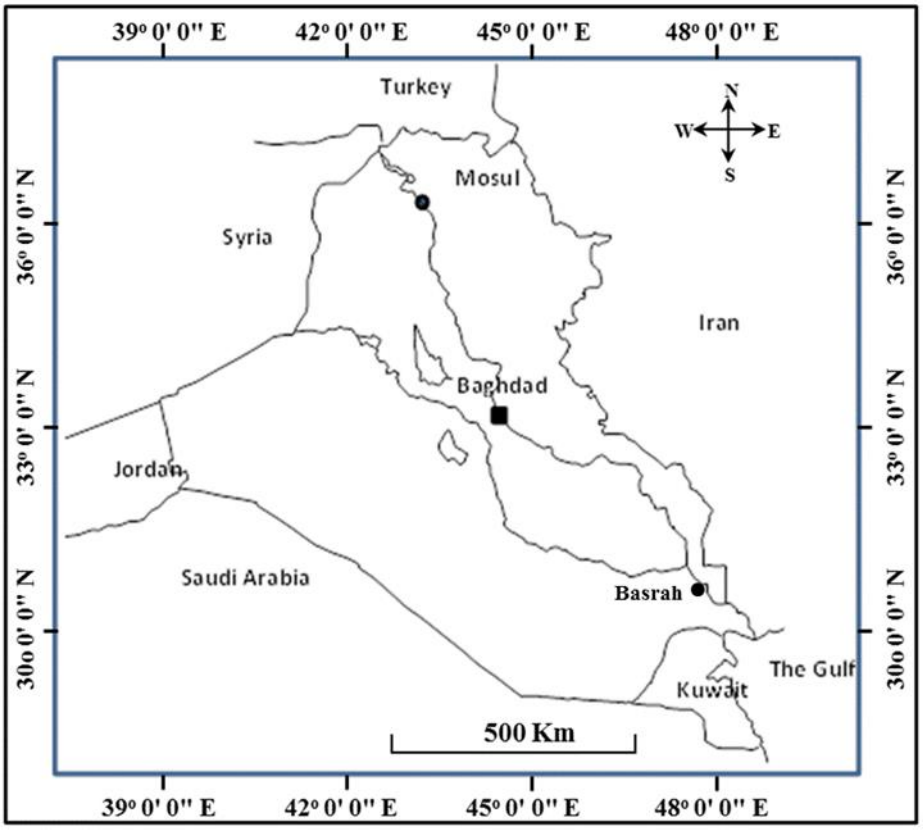


Figure 1. Map of Iraq showing the locations of Mosul and Baghdad.

2.2 Data sources and methods

Due to the lack of continuous monitoring stations in Mosul and Baghdad, this research relies on published real-time data of O_3 and NO_2 from an online platform from January 1, 2022, to December

31, 2022. The hourly concentrations of O_3 and NO_2 were collected along the study year using an air quality monitoring website (https://air.plumelabs.com/en/).

Hourly weather parameters data for Mosul and Baghdad were obtained from the website https://www.meteoblue.com/weather/archive/export including temperature (T), relative humidity (RH), wind speed (WS), wind direction (WD), cloud cover high (CCH), cloud cover median (CCM), cloud cover low (CCL), sunshine duration (SSD), short wave radiation (SWR), UV radiation (UV), atmospheric pressure (AP) and precipitation (P).

2.3 Statistical analysis

Descriptive statistics were employed, including the mean, median, standard deviation, and range. The data were statistically analyzed using nonparametric tools. The Kruskal-Wallis and pairwise Mann-Whitney tests were utilized to detect monthly and seasonal variations for O_3 and NO_2. Additionally, the Mann-Whitney test was used to examine the differences between Mosul and Baghdad. The number and percentage of polluted days in Mosul and Baghdad were reported in accordance with WHO guidelines. The difference in polluted days between Mosul and Baghdad was tested using the Chi-square test.

To assess short-term NO_2 levels according to WHO (2021) guidelines, daily 24-hour mean concentrations were computed from the hourly dataset. Compliance was evaluated against the 25 $\mu g/m^3$ threshold using the 99th percentile metric, which restricts the allowable exceedances to no more than 3–4 days per calendar year. Daily short-term exposure to O_3 was evaluated by extracting the daily maximum 8-hour running average for each day of the year (365 values) and comparing them against the WHO (2021) AQG benchmark of 100 $\mu g/m^3$. Compliance was defined according to the 99^{th} percentile requirement, which permits a maximum of 3–4 exceedance days per year. The long-term health risk was evaluated using the WHO peak season metric, defined as the average of daily maximum 8-hour mean O_3 concentrations during the six consecutive months with the highest running average. The recorded peak season concentration was compared with WHO AQG level (60 $\mu g/m^3$) and the Interim Target 1 (100 $\mu g/m^3$).

The relationships between O_3 and NO_2 and meteorological parameters were analyzed using multiple linear regression analysis. The standardized regression coefficient (β) was used to estimate the power of the meteorological parameters.

3. Results and discussion

3.1 Nitrogen dioxide (NO_2)

The monthly mean NO_2 concentrations in Mosul city for 2022 exhibited temporal fluctuations, ranging from 9.8 $\mu g/m^3$ (median: 6 $\mu g/m^3$) in the hot month of June to 34.7 $\mu g/m^3$ (median: 36 $\mu g/m^3$)

ACCEPTED MANUSCRIPT

in the cold month of December (**Table 1**). This temporal variation resulted in an annual average of 21.2 μg/m^3 (median: 18 μg/m^3), which is approximately double the annual World Health Organization (WHO) Air Quality Guidelines (AQG) of 10 μg/m³ for long term exposure (Hoffmann *et al*., 2021; WHO, 2022). In comparison, Baghdad has a higher baseline; its lowest monthly mean, recorded in July, was 22.5 μg/m^3 (median: 16 μg/m^3), more than twice the minimum of Mosul. The maximum concentration in Baghdad occurred in December, was 50.9 μg/m^3 (median: 52 μg/m^3), which is more than 1.5 times that of Mosul. Therefore, Baghdad's annual NO_2 average of 36.7 μg/m³ (median: 34 μg/m^3), exceeding the WHO AQG for long term exposure by more than 3.5 times. This elevated trend in the capital coincided with Mohammed *et al*. (2019), who justify the reason of high NO_2 levels to dense motor vehicle traffic. This difference is further driven by Baghdad's hyper-urbanized environment, higher population density, industrial activities and heavier traffic volumes compared to Mosul (Chaichan *et al*., 2018; Mohammed *et al*., 2019), all of which release substantial amounts of NO_x emissions.

For short term exposure, the 99th percentile for mean daily NO_2 concentrations was 44.73 μg/m^3 for Mosul city, and 73.9 μg/m^3 for Baghdad, with 3 and 2 exceedance days for Mosul and Baghdad respectively, indicating full alignment with WHO short term air quality guidelines.

Table 1. Descriptive statistics of NO_2 concentrations for Mosul and Baghdad cities with comparison according to month (μg/m³)

Cities	**Mosul**				**Baghdad**				**p-value**
Months	**Median**	**Mean**	**SD**	**Range**	**Median**	**Mean**	**SD**	**Range**	
Jan	26.0^{e}	27.7	13.5	3.0-62.0	43.0^{g}	42.6	14.0	8.0-85.0	<0.001
Feb	27.0^{e}	27.7	16.0	3.0-67.0	40.0^{f}	39.5	15.0	7.0-90.0	<0.001
Mar	17.0^{c}	19.3	13.5	1.0-85.0	34.0^{e}	35.1	15.8	6.0-86.0	<0.001
Apr	20.0^{d}	22.6	16.8	1.0-74.0	36.0^{f}	40.3	21.6	6.0-93.0	<0.001
May	8.0^{b}	13.3	13.0	1.0-57.0	24.0^{c}	30.5	20.5	5.0-84.0	<0.001
Jun	6.0^{a}	9.8	10.2	1.0-59.0	20.0^{b}	26.4	19.9	4.0-122.0	<0.001
Jul	7.0^{b}	12.6	12.9	1.0-58.0	16.0^{a}	22.5	16.4	4.0-92.0	<0.001
Aug	8.0^{b}	11.5	11.2	1.0-61.0	20.0^{b}	26.2	18.4	7.0-122.0	<0.001
Sep	17.0^{c}	18.8	13.1	1.0-72.0	29.0^{d}	33.5	18.7	7.0-89.0	<0.001
Oct	26.0^{e}	28.7	17.7	2.0-74.0	45.0^{g}	46.3	21.3	7.0-157.0	<0.001
Nov	29.0^{e}	28.7	16.1	2.0-65.0	49.0^{h}	47.5	15.7	12.0-88.0	<0.001
Dec	36.0^{f}	34.7	13.5	6.0-74.0	52.0^{i}	50.9	15.7	13.0-104.0	<0.001
Annual	**18.0**	**21.2**	**16.2**	**1.0-85.0**	**34.0**	**36.7**	**20.0**	**4.0-157.0**	<0.001

All values in μg/m^3, SD = Standard deviation. Each letter in the numbers represents a statistical level. Medians with different letters vertically have significant differences at $p \leq 0.05$ according to Kruskal-Wallis and Mann-Whitney tests.

As showed in **Figure 2**, both cities experienced a marked pattern, with peak NO_2 concentrations occurring during the colder months (winter and autumn) and falling during summer. The seasonal variation may be attributed to three factors: (1) increased anthropogenic emissions during colder months from heating and combustion processes; (2) the prolonged atmospheric life-time NO_2 during

ACCEPTED MANUSCRIPT

winter as a result of reduced photochemical activity and lower solar intensity, which slows down the photodissociation rate of NO_2 (Cichowicz *et al*., 2017; Al-Sultan *et al*., 2022) and (3) meteorological pressing, specially frequent winter thermal inversions and shallow Planetary Boundary Layer Height (BPLH). Cold ground temperatures prevent vertical atmospheric mixing and catching emitted pollutants close to surface. This seasonal action is agreed with the local findings of Shihab and Al-Jarrah (2015).

On a daily basis, Mosul experienced 129 days in 2022 where NO_2 levels exceeded the 24-hour WHO AQG standard (25 µg/m^3), whereas Baghdad recorded a staggering 285 exceedance days. The great majority of these exceedances were strongly clustered during the winter and autumn seasons in Mosul, compared to winter, spring and autumn in Baghdad, as detailed in **Table 2**.

.

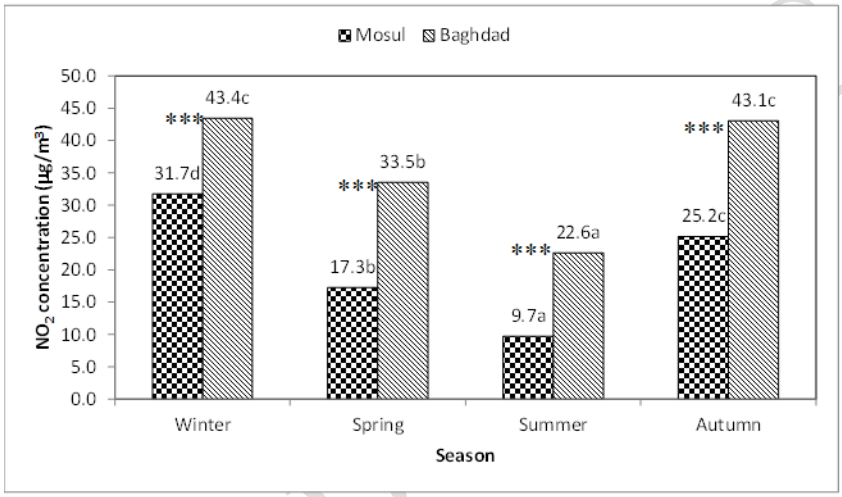


Figure 2. Seasonal variation of NO_2 in Mosul and Baghdad cities

Significant difference according to season ($p < 0.001$) using Kruskal–Wallis test and Mann-Whitney pairwise test for Mosul and Baghdad cities. The letters on the bars indicate the seasonal difference statistically ($p < 0.05$) for each town alone (sharing the same letter between any two non-adjacent bars (seasons) means no significant difference).

••• noted Significant difference between Mosul and Baghdad ($p < 0.001$) using the Mann -Whitney test

3.2 Ozone (O_3)

Descriptive statistics for ambient O_3 in 2022 (**Table 3**) revealed a pronounced summer-high and winter-low pattern typical of arid and semi-arid regions. In Mosul, monthly averages swung from a winter minimum of 21.5 µg/m^3 (median: 13 µg/m^3) in December to a summer peak of 91.2 µg/m^3 (median: 88 µg/m^3), with an annual mean of 58.1 µg/m^3 (median: 55 µg/m^3). Baghdad's levels extended from 16.7 µg/m^3 (median: 11 µg/m^3) in December to 87.7 µg/m^3 (median: 83 µg/m^3) in July, resulting in a lower annual average of 53.1 µg/m^3 (median: 47.0 µg/m^3). This seasonal outline (**Figure 3**) is guided by variations in solar zenith angles and temperatures that control the photolytic rates of NO_2 required to support tropospheric ozone production (Nguyen *et al*., 2022; Hachim *et al*., 2024a).

ACCEPTED MANUSCRIPT

The highest peak season concentrations for ozone were 111.8 and 108.9 μg/m^3 found in May to October for Mosul and Baghdad respectively. This value exceeding the WHO AQG (60 μg/m^3) and the Interim Target 1 (100 μg/m^3). This elevated peak season confirms continuation of photochemical activity in the warmer months.

Table 2. Monthly distribution of NO_2 short-term exposure according to the 24-hour WHO global air quality guidelines (AQG) in Mosul and Baghdad

Cities	Mosul				Baghdad			
WHO AQG	≤25 μg/m^3		>25 μg/m^3		≤25 μg/m^3		>25 μg/m^3	
Months	No.	%	No.	%	No.	%	No.	%
Jan	13	41.9	18	58.1	1	3.2	30	96.8
Feb	10	35.7	18	64.3	1	3.6	27	96.4
Mar	25	80.6	6	19.4	2	6.5	29	93.5
Apr	21	70.0	9	30.0	4	13.3	26	86.7
May	31	100	0	0.0	9	29.0	22	71.0
Jun	30	100	0	0.0	16	53.3	14	46.7
Jul	31	100	0	0.0	22	71.0	9	29.0
Aug	30	96.8	1	3.2	20	64.5	11	35.5
Sep	25	83.3	5	16.7	5	16.7	25	83.3
Oct	9	29.0	22	71.0	0	0.0	31	100.0
Nov	10	33.3	20	66.7	0	0.0	30	100.0
Dec	1	3.2	30	96.8	0	0.0	31	100.0
Total	236	64.7	129	35.3	80	21.9	285	78.1
Significance	<0.001				<0.001			

Table 3. Descriptive statistics of monthly O_3 concentrations with comparison for Mosul and Baghdad (μg/m^3)

Months	Mosul				Baghdad				p-value
	Median	Mean	SD	Range	Median	Mean	SD	Range	
Jan	28.0^{b}	29.1	20.0	1.0-78.0	20.0^{b}	22.6	17.4	0.0-74.0	<0.01
Feb	33.5^{c}	38.3	26.6	1.0-99.0	31.0^{d}	34.8	21.6	0.0-96.0	>0.05 NS
Mar	49.5^{d}	50.2	25.6	1.0-105.0	42.0^{e}	44.1	22.7	3.0-95.0	<0.01
Apr	55.0^{e}	56.9	29.6	5.0-121.0	48.0^{f}	57.0	47.0	5.0-137.0	>0.05 NS
May	77.0^{g}	74.7	31.2	8.0-139.0	68.0^{g}	68.2	34.5	1.0-147.0	<0.01
Jun	85.0^{h}	82.5	28.7	11.0-160.0	72.0^{h}	76.1	34.0	4.0-158.0	0.01
Jul	88.0^{i}	91.2	34.7	5.0-163.0	83.0^{j}	87.7	31.7	4.0-167.0	>0.05 NS
Aug	81.0^{hi}	85.9	32.4	10.0-166.0	74.0^{i}	80.4	33.5	9.0-179.0	<0.05
Sep	66.0^{f}	71.5	33.8	1.0-168.0	60.0^{g}	68.2	32.3	7.0-162.0	>0.05 NS
Oct	45.0^{d}	54.2	32.8	5.0-137.0	42.0^{e}	47.3	29.2	1.0-137.0	<0.05
Nov	33.5^{c}	40.0	26.5	3.0-98.0	26.0^{c}	31.0	22.1	2.0-96.0	0.001
Dec	13.0^{a}	21.5	20.3	1.0-74.0	11.0^{a}	16.7	16.8	1.0-70.0	<0.001
Annual	**55.0**	**58.1**	**36.5**	**0.0-168.0**	**47.0**	**53.1**	**37.4**	**0.0-390.0**	<0.01
NS: not significant.									

The seasonal patterns for both cities exhibit a consistent temporal tendency. The minimum values of winter sides with Hachim *et al*. (2024a), led by lesser solar zenith angles, shorter daylight hours, and

ACCEPTED MANUSCRIPT

lower temperatures that together overcome the NO_2 photolysis rates necessary to maintain tropospheric ozone production. On the other hand, warming and extended photoperiods during spring enable the recovery of O_3 synthesis. This leads to higher summer peaks-averaging 87.0 µg/m^3 in Mosul and 82.2 µg/m^3 in Baghdad-where intense shortwave solar radiation and high thermal coverings speed up photochemical kinetics, a trend agreed with international literature (de Souza *et al*., 2025; Wang *et al*., 2025).

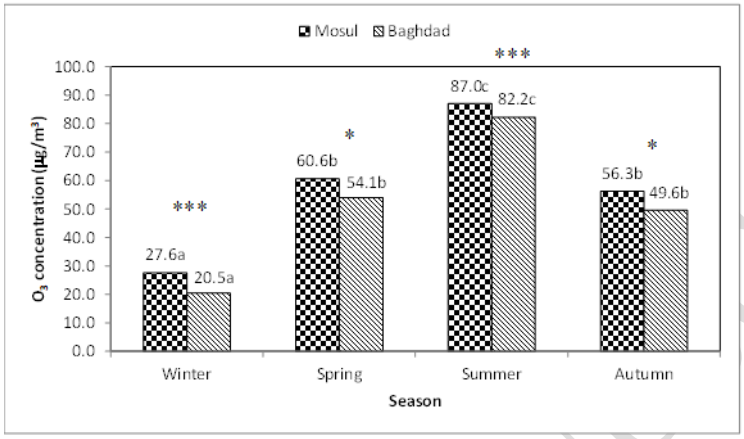


Figure 3. Seasonal means of O_3 concentration in Mosul and Baghdad cities with comparison

* the difference is significant at ($p \leq 0.001$) Kruskal–Wallis and Mann Whitney pairwise test. Different letters on non-adjacent bars = statistical difference ($p \leq 0.05$) for each town
••• significant difference between cities at ($p < 0.001$) Mann Whitney test.

A spatial inconsistency was observed: although Baghdad recording higher NO_2 concentrations (**Table 1, Figure 2**), its local O_3 levels were lower than Mosul's. This inverse relationship is regulated by two primary atmospheric processes: (1) The ozone titration effect: Baghdad's heavy traffic volume and industrial emissions produce heavy fluxes of nitric oxide (NO). In this heavily polluted urban area, O_3 is rapidly consumed via the classic titration pathway to produce NO_2 and molecular oxygen (O_2) (Cooper and Alley, 2010; de Souza *et al*., 2025): $NO + O_3 \rightarrow NO_2 + O_2$. This localized chemical sink reduces net O_3 accumulation in Baghdad's high-traffic core, while Mosul's lower NO emissions limit allows generated O_3 to persist (Shihab, 2022). (2) Topographic and barometric influences: Mosul's higher geographic elevation relates with a lower mean atmospheric pressure reference. Lower surface barometric pressures are frequently related with enhanced downward move of ozone from the upper troposphere and margin layer dynamics that prefer higher surface O_3 accumulation (Ilić *et al*., 2020).

For short term exposure, the 99th percentile for daily maximum 8-hours O_3 reached 152.88 µg/m^3 in Mosul city, and 146.12 µg/m^3 in Baghdad, with 3 exceedance days for the two cities, showing full alliance with WHO short term air quality guidelines.

ACCEPTED MANUSCRIPT

Although annual averages recommend overall compliance, evaluating short-term peaks versus the WHO AQG threshold (100 μg/m^3 for the daily maximum 8-hour mean) shows a critical human exposure risk. As detailed in **Table 4**, Mosul faced a cumulative total of 146 exceedance days, mostly clustered between April and September, with high incidences in May (20 days) and June (26 days). Baghdad recorded 135 exceedance days, presenting a stricter temporal concentration during hyper-arid peak summer months of June (28 days) and July (31 days). This high rate of noncompliance points out a serious photochemical smog threat in the dry season, showing that compliant annual means can hide acute seasonal exposure hazards.

Table 4. Monthly distribution of short-term exposure to O_3 according to the 8-hour daily WHO global air quality guidelines (AQG) in Mosul and Baghdad

Cities	Mosul				Baghdad			
WHO AQG	≤100 μg/m^3		>100 μg/m^3		≤100 μg/m^3		>100 μg/m^3	
Months	No.	%	No.	%	No.	%	No.	%
Jan	31	100.0	0	0.0	31	100.0	0	0.0
Feb	28	100.0	0	0.0	28	100.0	0	0.0
Mar	31	100.0	0	0.0	31	100.0	0	0.0
Apr	23	76.7	7	23.3	26	86.7	4	13.3
May	11	35.5	20	64.5	11	35.5	20	64.5
Jun	4	13.3	26	86.7	2	6.7	28	93.3
Jul	1	3.2	30	96.8	0	0.0	31	100.0
Aug	1	3.2	30	96.8	0	0.0	31	100.0
Sep	7	23.3	23	76.7	12	40.0	18	60.0
Oct	21	67.7	10	32.3	28	90.3	3	9.7
Nov	30	100.0	0	0.0	30	100.0	0	0.0
Dec	31	100.0	0	0.0	31	100.0	0	0.0
Total	219	60.0	146	40.0	230	63.0	135	37.0
Significance	<0.001				<0.001			

3.3 Diurnal and weekly variations of NO_2 and O_3

The temporal dynamics of NO_2 and O_3 in Mosul and Baghdad show a common reciprocal photochemical link illustrated by highly uncorrelated diurnal outlines. In Mosul (**Figure 4**), NO_2 shows a apparent bimodal distribution with a obvious morning rush-hour peak (06:00–08:00 LT), followed by a sharp daytime depletion (< 10 μg/m^3) between 12:00 and 15:00 LT due to extreme photolysis, which at the same time pushes secondary O_3 concentrations to crest above 95 μg/m^3. An obvious weekend effect occurs on Fridays in Mosul, where daytime NO_2 falls to the lowest weekly limit due to low traffic volume, but afternoon O_3 stays high due to reduced ozone-scavenging titration ($NO + O_3 \rightarrow NO_2 + O_2$). This weekend ozone response associate with local evaluation in Mosul (Shihab and Al-Jarrah, 2015). Comparative analysis with Baghdad (**Figure 5**) shows basic variations in urban atmospheric chemistry. Baghdad exhibiting a significantly higher limit for both pollutants

ACCEPTED MANUSCRIPT

within the week. Also, nighttime and rush-hour NO_2 peaks commonly exceed 50 μg/m^3 and its midday minimum remains elevated at ~20 μg/m^3, encouraging photochemical cycle to pushe daytime O_3 peaks well above 115 μg/m^3 due to heavy vehicular passes and industrial complexes like Al-Daura refinery. This permanent reservoir of precursors in Baghdad confirms the findings of Hashim *et al*. (2021), who mentioned that heavy dependence on private power generators and heavy traffic volumes maintains elevated emissions even during periods of lower commercial activities. Furthermore, nighttime O_3 is effectively depleted to ~ 35 μg/m^3 in Mosul via overnight titration, whereas Baghdad maintains an elevated baseline above 65 μg/m^3. This prolonged excess ozone in Baghdad, even during Friday weekend, which indicates a stagnant atmospheric boundary layer and a complex VOC-limited chemical regime similar to megacity environments (Sillman, 1999), where high precursor density constrains the efficacy of temporary emission reductions.

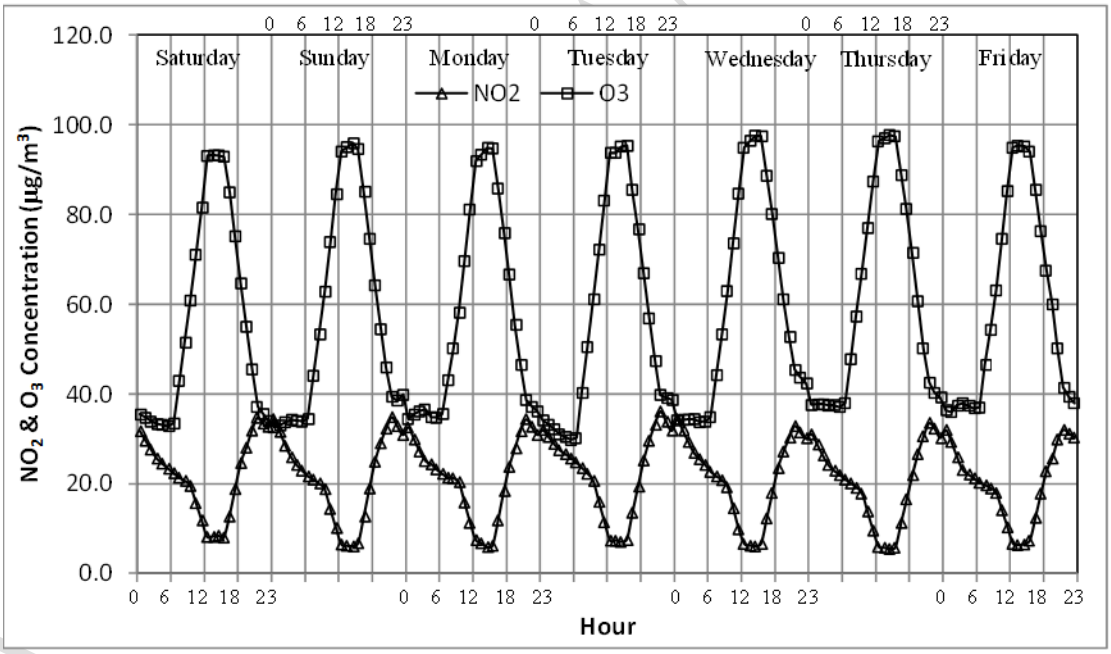


Figure 4. Annual hourly average diurnal variation of NO_2 and O_3 in Mosul city along weekdays

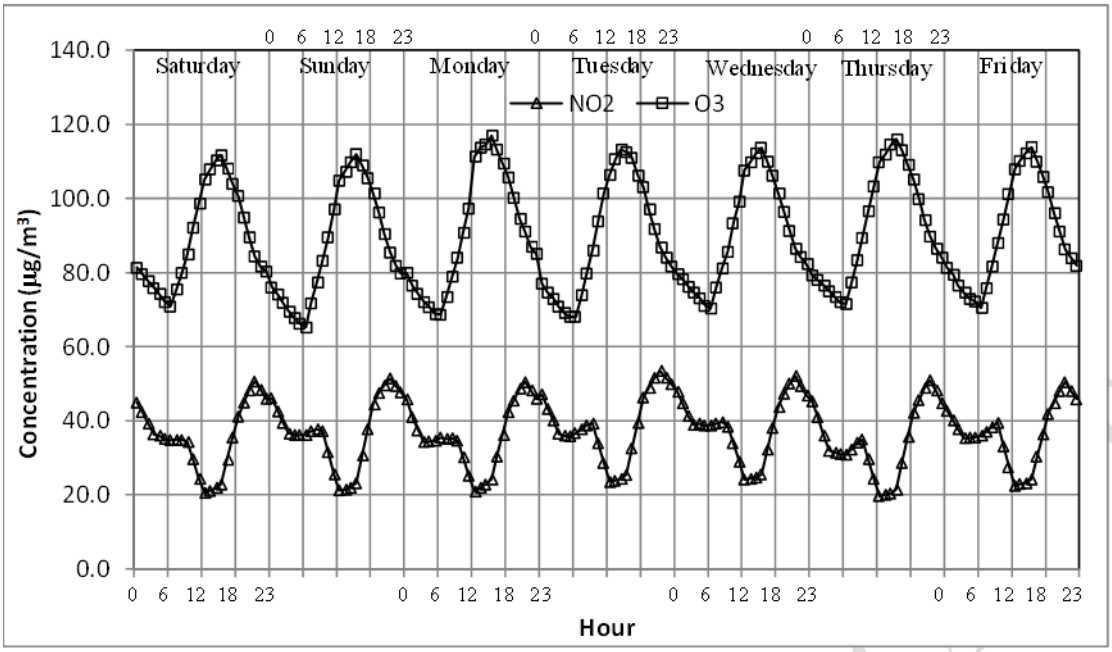


Figure 5. Annual hourly average diurnal variation of NO_2 and O_3 in Baghdad city along weekdays

3.4 Effect of meteorological parameters on NO_2 dynamics

Multiple linear regression was used to examine the effects of meteorological factors on ambient NO_2 concentrations in Mosul and Baghdad (**Tables 5 and 6**), with predictor importance classified by standardized regression coefficients (β) and p-values.

Table 5. Analysis of NO_2 concentrations and meteorological parameters Mosul city using multiple regression

Parameters	β	Standardized β	t-value	p-value
Temperature	-0.165	-0.161	-6.874	<0.001
Relative humidity	0.021	0.039	1.980	0.048
Wind speed	-0.987	-0.371	-32.515	<0.001
Wind direction	-0.014	-0.120	-11.905	<0.001
Cloud cover	-0.084	-0.101	-4.44	<0.001
Cloud cover high	0.059	0.078	10.83	<0.001
Cloud cover medium	-0.025	-0.027	-1.584	0.113*
Cloud cover low	-0.055	-0.033	-4.008	<0.001
Sunshine duration	-0.139	-0.193	-17.66	<0.001
Short wave radiation	-0.045	-0.641	-7.069	<0.001
UV radiation	0.254	0.401	4.584	<0.001
Atmospheric pressure	0.044	1.665	43.896	<0.001
Precipitation	-2.585	-0.018	-3.446	0.001

* Not significant

ACCEPTED MANUSCRIPT

Table 6. Analysis of NO_2 concentration and meteorological parameters for Baghdad city using multiple regression

Parameters	β	Standardized β	t-value	p-value
Temperature	0.065	0.044	2.418	0.020
Relative humidity	0.080	0.080	6.193	<0.001
Wind speed	-1.387	-0.469	-44.031	<0.001
Wind direction	-0.003	-0.019	-1.763	0.080*
Cloud cover	0.082	0.044	2.294	0.020
Cloud cover high	0.046	0.036	4.647	<0.001
Cloud cover medium	-0.081	-0.038	-2.739	0.010
Cloud cover low	-0.127	-0.030	-4.515	<0.001
Sunshine duration	-0.020	-0.019	-1.948	0.050
Short wave radiation	0.007	0.062	0.618	0.540*
UV radiation	-0.217	-0.228	-2.349	0.020
Atmospheric pressure	0.054	1.309	45.548	<0.001
Precipitation	1.385	0.005	1.202	0.230*

* Not significant

3.4.1 Synoptic scale and dispersion drivers (pressure and wind speed)

Atmospheric pressure was the highest statistically significant direct predictor of NO_2 concentrations in Mosul and Baghdad (**Table 7**). High-pressure systems confine the planetary boundary layer height (PBLH), lessen vertical mixing, and increase atmospheric stability, thus blocking vehicular and industrial emissions and plugging NO_2 accumulation (Gasmi *et al*., 2017; Yildizhan *et al*., 2024).

In contrast, wind speed (WS) showed a significant inverse correlation with NO_2 in both cities, with a stronger effect in Baghdad. The city's flat terrain and open arid facilitating enable efficient dispersion of pollutants, while stronger winds increase turbulence and advection, speeding the dilution and movement of emissions away from urban areas (Jones *et al*., 2010; Román-Cascón *et al*., 2023).

Table 7. Significant meteorological parameters on NO_2 concentrations in Mosul and Baghdad with rating

Mosul			**Baghdad**		
Parameter	**Standardized β**	**p-value**	**Parameter**	**Standardized β**	**p-value**
Atmospheric pressure	1.665	<0.001	Atmospheric pressure	1.309	<0.001
Short wave radiation	-0.641	<0.001	Wind speed	-0.469	<0.001
UV radiation	0.401	<0.001	UV radiation	-0.228	0.02
Wind speed	-0.371	<0.001	Relative humidity	0.080	<0.001
Sunshine duration	-0.193	<0.001	Cloud cover	0.044	0.02
Temperature	-0.161	<0.001	Temperature	0.044	0.02
Cloud cover	-0.101	<0.001			
Relative humidity	0.039	0.048			
Precipitation	-0.018	0.001			

ACCEPTED MANUSCRIPT

3.4.2. Photochemical radiative forcing

Radiative parameters varying highly the site-specific photochemical dynamics due to emission baselines fluctuation:

Shortwave Radiation (SWR) & Sunshine Duration: Shortwave radiation (SWR) was the second strongest predictor in Mosul, through a significant inverse relationship with NO_2 by enhancing photolysis, which converts NO_2 to NO and supports tropospheric O_3 formation, and reduces NO_2 concentrations (Seinfeld & Pandis, 2016). Also, sunshine duration was inversely related with NO_2 in Mosul ($\beta = -0.139$, $p < 0.001$), showing enhanced photolysis and convective mixing. In contrast, sunshine duration had only a slight effect in Baghdad ($\beta = 0.020$, $p = 0.05$), where continuous anthropogenic emissions largely balance the atmosphere's natural self-cleansing capacity (Lelieveld *et al*., 2015).

UV Radiation: UV radiation showed a strong positive correlation with NO_2 in Mosul ($\beta = 0.254$, $p<0.001$). Conversely, this relationship inverted into a significant inverse correlation in Baghdad ($\beta= -0.217$, $p = 0.020$). Given Baghdad's heavy, stagnant reservoir of NO_2 from millions of vehicles and diesel generators (Chaichan *et al.*, 2018), elevated UV intensities originate intense direct photolysis ($NO_2 + h\nu \rightarrow NO + O$), acting mainly as a chemical sink (Finlayson-Pitts and Pitts Jr., 2000).

3.4.3 Micro-climate and thermodynamic controls

Precipitation (Wet Scavenging): Precipitation showed different effects between Mosul and Baghdad. In Baghdad, the correlation with NO_2 was weak and non-significant ($\beta = 0.005$, $p = 0.230$), indicating that limited rainfall is not enough for effective wet scavenging (Zhao *et al*., 2020). While, Mosul presented a significant negative association ($\beta = -0.018$, $p = 0.001$), with more effective pollutant removal under its more wetter Mediterranean-influenced climate (Zakaria *et al*., 2013).

Cloud cover also showed a negative association with NO_2 in Mosul ($\beta = -0.084$, $p < 0.001$), which may be due to enhanced atmospheric mixing during forward systems, whereas in Baghdad its effect was positive by reducing photolysis and blocking the planetary boundary layer height (PBLH), and promoting pollutant accumulation (Lelieveld *et al*., 2015).

Temperature & Relative Humidity: Temperature showed different effect on NO_2 in the two cities. In Mosul, it was significant and negatively correlated with NO_2 ($\beta = -0.161$, $p = 0.001$), enhanced with thermal convection and photolysis during warmer periods (Schäfer *et al*., 2012). In Baghdad, however, temperature showed a significant positive correlation ($\beta = 0.044$, $p = 0.020$), probably due to increased traffic and diesel generator emissions during extreme heat, outweighing atmospheric dispersion (Vardoulakis *et al*., 2003). Relative humidity (RH) was positively correlated with NO_2 in

ACCEPTED MANUSCRIPT

both Mosul (β = 0.044, p = 0.020) and Baghdad (β = 0.080, p < 0.001), indicating more stable atmospheric conditions, weaker winds, and reduced photolysis (He *et al*., 2017).

3.5 Spatiotemporal dynamics and photochemical pathways of ozone (O_3)

3.5.1 Meteorological drivers of ozone dynamics

Temperature: Ambient temperature was the most dominant driver of O_3 dynamics in both cities, attaining the highest standardized coefficients (**Tables 8-10**) in Mosul (β = 0.577, p < 0.001) and Baghdad, (β = 0.667, p < 0.001). Excessive thermal conditions directly accelerate the kinetic reaction rates of the photochemical smog cycle and generate large evaporative emissions of anthropogenic VOCs, shifting the equilibrium toward accelerated O_3 formation within stagnant anticyclonic systems (Bloomer *et al.*, 2009).

Radiation Parameters (SWR, UV, and Sunshine Duration): Radiation parameters in Mosul and Baghdad affected O_3 formation in a different way. In Mosul, SWR was the second strongest positive predictor (β = 0.34, p < 0.001), supplying the energy required for NO_2 photolysis (Tang *et al.*, 2009). In contrast, SWR was not significant in Baghdad (β = −0.008, p > 0.05) due to aerosol dimming caused by traffic and diesel-generator emissions (Salman and Hassan, 2026; Li *et al.*, 2022). On the other hand, UV radiation became the second strongest predictor (β = 0.246, p < 0.001), while in Mosul it showed a weak inverse effect (β = −0.097, p = 0.05), probably indicating midday photochemical saturation (Hachim *et al.*, 2024b). Sunshine duration stayed a significant positive component in both cities (p < 0.001), with a stronger effect in Mosul (β = 0.114) than in Baghdad (β = 0.033) because of lower aerosol attenuation (Feng and Wang, 2021).

Table 8. Results of multiple regression analysis for O_3 and meteorological parameters for Mosul city

Parameters	β	Standardized β	t-value	p-value
Temperature	1.525	0.577	43.048	<0.001
Relative humidity	-0.078	-0.056	-4.946	<0.001
Wind speed	0.834	0.122	18.635	<0.001
Wind direction	0.009	0.032	5.567	<0.001
Cloud cover	0.176	0.082	6.272	<0.001
Cloud cover high	-0.081	-0.042	-10.14	<0.001
Cloud cover medium	0.047	0.02	1.992	0.050
Cloud cover low	-0.013	-0.003	-0.652	0.52*
Sunshine duration	0.211	0.114	18.165	<0.001
Short wave radiation	0.062	0.34	6.543	<0.001
UV radiation	-0.158	-0.097	-1.936	0.050
Atmospheric pressure	-0.001	-0.021	-0.959	0.34*
Precipitation	8.427	0.023	7.625	<0.001

* Not significant

ACCEPTED MANUSCRIPT

Table 9. Results of multiple regression analysis for O_3 and meteorological parameters for Baghdad city

Parameters	β	Standardized β	t-value	p-value
Temperature	1.519	0.667	42.077	<0.001
Relative humidity	-0.113	-0.073	-6.461	<0.001
Wind speed	1.200	0.261	28.258	<0.001
Wind direction	-0.004	-0.016	-1.691	0.090*
Cloud cover	-0.063	-0.022	-1.318	0.190
Cloud cover high	-0.049	-0.024	-3.651	<0.001
Cloud cover medium	0.125	0.038	3.126	<0.001
Cloud cover low	0.129	0.020	3.404	<0.001
Sunshine duration	0.056	0.033	3.944	<0.001
Short wave radiation	-0.008	-0.047	-0.537	0.590*
UV radiation	0.390	0.264	3.136	<0.001
Atmospheric pressure	-0.007	-0.107	-4.291	<0.001
Precipitation	-0.164	0.000	-0.105	0.920*

* Not significant

Wind Speed & Atmospheric Pressure: Wind speed (WS) is ranked third in both cities. It influenced O_3 concentration through different mechanisms. In Baghdad, WS had a strong positive effect on O_3 ($\beta = 0.261$, $p < 0.001$), through improving boundary-layer mixing, upper-tropospheric O_3 intrusion, and local transport of aged pollution plumes (Klein *et al.*, 2014; Caputi *et al.*, 2019). In Mosul, it has weaker effect ($\beta = 0.122$), offering a balance between maintaining background O_3 levels and slight pollutant dilution (Seinfeld and Pandis, 2016). Atmospheric pressure revealed a significant inverse relationship in Baghdad ($\beta = -0.107$, $p < 0.001$), showing the influence of low-pressure systems on atmospheric stability and precursor collection. On the other hand, pressure was not significant in Mosul (Rank 12, $\beta = -0.021$) due to complicated terrain and local motion patterns that reduce the effect of synoptic pressure variations (Demuzere *et al.*, 2009; Stohl *et al.*, 2003).

Table 10. Significant meteorological parameters on O_3 concentration in Mosul and Baghdad

Mosul			Baghdad		
Parameter	**Standardized β**	**p-value**	**Parameter**	**Standardized β**	**p-value**
Temperature	0.577	<0.001	Temperature	0.667	<0.001
Short Wave Radiation	0.340	<0.001	UV Radiation	0.264	<0.001
Wind Speed	0.122	<0.001	Wind Speed	0.261	<0.001
Sunshine Duration	0.114	<0.001	Atmospheric Pressure	-0.107	<0.001
UV Radiation	-0.097	0.050	Relative Humidity	-0.073	<0.001
Cloud Cover	0.082	<0.001	Cloud Cover Medium	0.038	<0.001
Relative Humidity	-0.056	<0.001	Sunshine Duration	0.033	<0.001
Cloud Cover High	-0.042	<0.001	Cloud Cover High	-0.024	<0.001
Wind Direction	0.032	<0.001	Cloud Cover Low	0.020	<0.001
Precipitation	0.023	<0.001			
Cloud Cover Medium	0.020	0.05			

ACCEPTED MANUSCRIPT

3.6 Literature validation and environmental context

There is a strong agreement between the statistical finding of this study and the previous urban air quality studies. The role of mechanical dispersion in reducing initial emissions was confirmed by the inverse relationship between WS and NO_2 (Abbood *et al.*, 2025). Meanwhile, the positive effect of temperature and radiation on O_3 agrees with observations in high-solar-radiation areas (Wang *et al.*, 2026). The observed transport pattern also supports secondary pollutant behavior reported by Zhang *et al.* (2020), specifying that while regional meteorology controls photochemical processes ($\beta > 0.50$ for O_3), local geography and industrial sources determine pollutant distribution and peak concentrations.

3.7 Spatial and directional dynamics

In Mosul, the wind direction regulates extreme air pollution incidents through a definite local meteorological signature.

The Bottom 30% Percentile (**Figure 6a**): Clean air intervals are made by two main wind sectors: a prominent north-to-northwesterly (N-NNW) flow-combining to the cleansing local Shamal winds-and a high-velocity (> 2 m/s) easterly-to-northeasterly (E–NNE) component, which may be supported by local topography. The absence of calm conditions (<1m/s) confirms that wind velocity drives mechanical turbulence and urban ventilation (Çelik *et al.*, 2026; Seinfeld & Pandis, 2016).

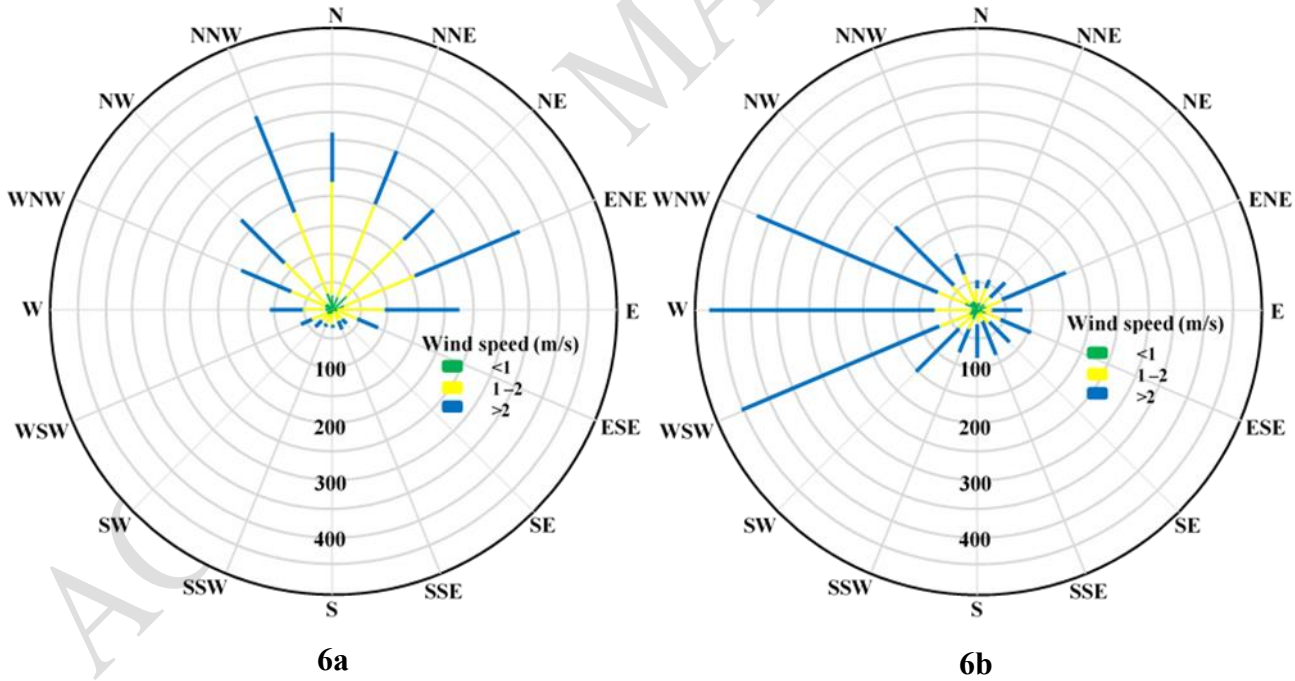


Figure 6. O_3 concentrations, wind direction and speed as a rose diagram for Mosul city, (a) for bottom 30% and (b) for top 30%

The Top 30% Percentile (Figure 6b): On the contrary, peak O_3 episodes show a sharp, main spatial clustering toward the western and southwestern sectors (W, WNW, and WSW). This peak pollution is regulated by a dual mechanism: high-velocity western winds act as a transport path into the urban

ACCEPTED MANUSCRIPT

center (Yang *et al*., 2025), while an increase in low wind speeds (<1 m/s) near the center supports local precursor accumulation.

In Baghdad, a pollution rose analysis was done for the bottom and top 30% of concentrations to understand the atmospheric mechanisms managing surface O_3.

The Bottom 30% Percentile (Figure 7a): Lower O_3 levels are predominantly accompanied with strong winds (> 2 m/s) from the northwest (NW) and west-northwest (WNW) zones. This indicates a strong "ventilation effect"; the high wind speeds develops mechanical turbulence and horizontal mixing, diluting surface O_3 and its precursors (NO_x and VOCs) (Seinfeld & Pandis, 2016). Besides, these air masses arise from less industrialized and open terrains upwind which feeding cleaner rural air into the capital (Clapp & Jenkin, 2001).

The Top 30% Percentile (**Figure 7b**): Peak O_3 occurrences remain side with the same NW and WNW paths but exhibit considerably higher frequency counts (stretching toward 600–800 thresholds). This shows a dual synoptic influence. Since the strong winds usually support dispersion, their association with peak O_3 points out regional photochemical transport. As a secondary pollutant, O_3 and its precursors undergo photochemical aging while being transported from upwind industrial zones northwest of Baghdad. This aligns with seasonal synchronicity in Iraq, where intense summer NW winds coincide with maximum solar radiation and excessive temperatures, converting these wind vectors into a carrier for locally peak-formed O_3 (Smoydzin *et al*., 2012; Hachim *et al*., 2024b).

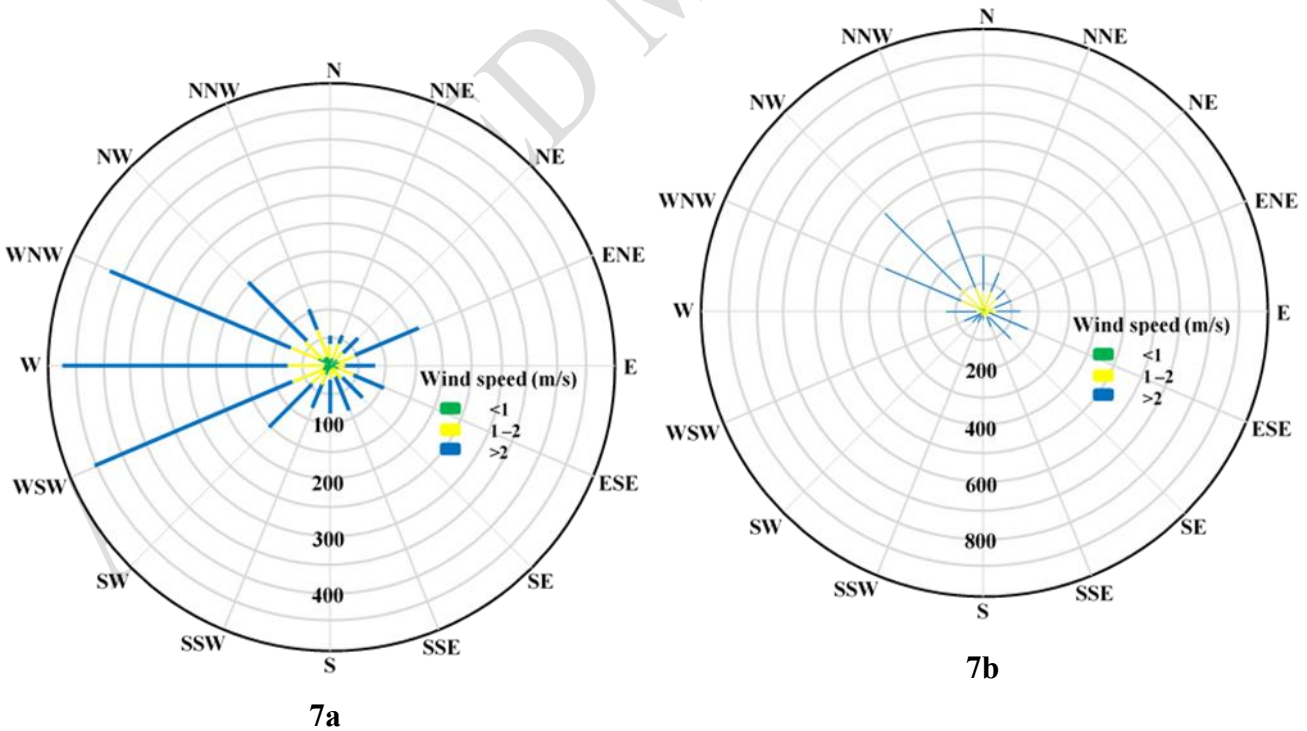


Figure 7. O_3 concentration, wind direction and speed as a rose diagram for Baghdad city, (a) for bottom 30% and (b) for top 30%

ACCEPTED MANUSCRIPT

4. Conclusions

1. NO_2 baseline was higher in Baghdad than Mosul (exceeding annual WHO guidelines by 3.5 vs. 2), guided by hyper-urbanization, dense traffic fleets, and widespread private generator use.
2. Mosul recorded lower surface O_3 concentrations due to rapid localized ozone titration ($NO + O_3 \rightarrow NO_2 + O_2$) than in Baghdad's high-traffic core, and Mosul's lower NO_x baseline allows greater O_3 persistence.
3. Anti-correlated seasonal trends were found in Mosul and Baghdad, with NO_2 peaking in winter due to boundary layer trapping and O_3 peaking in summer. High frequencies of daily exceedances for both pollutants emphasize acute seasonal smog risks masked by compliant annual averages.
4. The main positive drivers for NO_2 accumulation was atmospheric pressure and temperature for O_3 synthesis. While shortwave radiation drives O_3 photolysis in Mosul. High aerosol loading in Baghdad dissociates shortwave radiation, shifting the primary photochemical driver to UV radiation.
5. High-velocity regional northwesterly winds was associated with clean air in both cities. Conversely, peak O_3 occurrences are affected by local industrial movement from the west/southwest in Mosul, compared to local photochemical transport along the Tigris River basin in Baghdad.

References

1. Abbood, Z.M., Al-Jiboori, M.H., and Al-Taai, O.T. (2025). Impact of Aerosols on the Convective Boundary Layer Development over Baghdad City, *Iraqi Journal of Science,* ***66***(5), 2106-2117. https://doi.org/10.24996/ijs.2025.66.5.26
2. Abdipour, H., Narenji, M.A., Seyed Mousavi, S.E., Khammari, A., Ghnataghestani, M.D., Alijani, E., Kamani, H., Hosseinzehi, M. (2025). The relationship between biomarker interleukin-6 and particulate matter of dust storms (cohort study in 2024 – Zahedan city). *Toxicologie Analytique et Clinique*, ***37***(4): 504-512. https://doi.org/10.1016/j.toxac.2025.05.001
3. Abdipour, H., Seyed Mousavi, S.E., khammari, A., Alijani, E., Kamani, H. (2026). Evaluation of the relationship between C-reactive protein biomarker and particulate matter concentration from dust storms in Zahedan, Iran in 2024, *City and Environment Interactions*, ***29***, https://doi.org/10.1016/j.cacint.2026.100305.
4. Alnajm, D.J. (2023). *Spatial variation in the growth of the population of the governorates of Iraq for the period 2010-2020 and its expectations for the year 2030 AD. Russian Law Journal,* ***11***(3), 718–726.

ACCEPTED MANUSCRIPT

5. Al-Sultan, A.A., Al-Kindi, G.Y., Kadhim, R.J., and Al-Mhanawi, A.A.J. (2022). Assessment of the Ambient Gaseous Pollutants in the Crowded Traffic Crossroad in Baghdad City, *Ecological Engineering and Environmental Technology,* ***23***(5), 224–233. https://doi.org/10.12912/27197050/152140
6. Bloomer, B.J., Stehr, J.W., Piety, C.A., Salawitch, R.J., and Dickerson, R.R. (2009). Observed relationships of ozone air pollution with temperature and emissions, *Geophysical Research Letters,* ***36***(9), L09803. https://doi.org/10.1029/2009GL037308
7. Caputi, D.J., Faloona, I., Trousdell, J., Smoot, J., Falk, N., and Conley, S. (2019). Residual layer ozone, mixing, and the nocturnal jet in California's San Joaquin Valley, *Atmospheric Chemistry and Physics,* ***19***(7), 4721–4740. https://doi.org/10.5194/acp-19-4721-2019
8. Çelik, M.A., Bilik, A. and Akiner, M.E. (2026). Relation Between Air Quality and Wind Speed in the Eastern Anatolia Region of Türkiye, *Pure Applied Geophysics,* ***183***, 3159–3184. https://doi.org/10.1007/s00024-026-03994-1
9. Chaichan, M.T., Kazem, H.A., and Abed, T.A. (2018). Traffic and outdoor air pollution levels near highways in Baghdad, Iraq, *Environment, Development and Sustainability,* ***20***(2), 589–603. https://doi.org/10.1007/s10668-016-9900-x
10. Chatoutsidou, S.E., Kordonouri, I., and Lazaridis, M. (2026). An Air-Quality-Based Analysis of NO, NO_2, and O_3 at a Suburban Mediterranean Site, *Atmosphere,* ***17***(1), 7. https://doi.org/10.3390/atmos17010007
11. Chen, X., & Dai, A. (2024). Quantifying contributions of external forcing and internal variability to Arctic warming during 1900–2021. *Earth's Future*, ***12***, https://doi.org/10.1029/2023EF003734
12. Choi, Y., Song, M., Lee, Y., Paik, H.J., Song, J.S., Choi, Y. and Kim, D.H. (2024). Adverse effects of meteorological factors and air pollutants on dry eye disease: a hospital-based retrospective cohort study, *Scientific Reports,* ***14***, 17776. https://doi.org/10.1038/s41598-024-68070-x
13. Clapp, L.J., and Jenkin, M.E. (2001). Analysis of the relationship between ambient levels of O_3, NO_2 and NO as a function of NO_x in the UK, *Atmospheric Environment,* ***35***(36), 6391–6405. https://doi.org/10.1016/S1352-2310(01)00378-8
14. Cooper, C.D., and Alley, F.C. (2010). *Air pollution control: A design approach*. Waveland press. 4th ed., ISBN 13: 978-1-57766-678-3.
15. De Souza, A., de Oliveira-Júnior, J.F., Cardoso, K.R.A., and Gautam, S. (2025). Impact of vehicular emissions on ozone levels: A comprehensive study of nitric oxide and ozone interactions in urban areas, *Geosystems and Geoenvironment,* ***4***(1). https://doi.org/10.1016/j.geogeo.2024.100348

ACCEPTED MANUSCRIPT

16. Demuzere, M., Trigo, R.M., Vila-Guerau de Arellano, J., and van Lipzig, N.P.M. (2009). The impact of weather and atmospheric circulation on O_3 and PM_{10} levels at a rural mid-latitude site, *Atmospheric Chemistry and Physics,* ***9***(8), 2695–2714. https://doi.org/10.5194/acp-9-2695-2009
17. Encyclopedia Britannica. (2025). Iraq. https://www.Britannica.Com/Place/Iraq.
18. Feng, F. and Wang, K. (2021). Merging ground-based sunshine duration observations with satellite cloud and aerosol retrievals to produce high-resolution long-term surface solar radiation over China, *Earth System Science Data,* ***13***(3), 907-922. https://doi.org/10.5194/essd-13-907-2021
19. Finlayson-Pitts, B.J., and Pitts Jr, J.N. (2000). *Chemistry of the upper and lower atmosphere: Theory, experiments, and applications*. Academic Press. https://doi.org/10.1016/B978-012257090-2/50000-X
20. Gasmi, K., Aljalal, A., Al-Basheer, W., and Abdulahi, M. (2017). Analysis of NO_x, NO and NO_2 ambient levels as a function of meteorological parameters in Dhahran, Saudi Arabia, *WIT Transactions on Ecology and the Environment*, **211**, 77–86. https://doi.org/10.2495/AIR170081
21. Goldberg, D.L., Harkey, M., de Foy, B., Judd, L., Johnson, J., Yarwood, G., and Holloway, T. (2022). Evaluating NO_x emissions and their effect on O_3 production in Texas using TROPOMI NO_2 and HCHO, *Atmospheric Chemistry and Physics,* ***22***, 10875–10900, https://doi.org/10.5194/acp-22-10875-2022
22. Hachim, M.S., Rajab, J.M., and Al-Salihi, A.M. (2024a). Evaluation of the Trends Variance of Atmospheric Environment using "MAKESENS" Model with Spatiotemporal Seasonal Analysis over Iraq 2003-2021, *African J. Bio. Sci,* ***6***(6), 118–133. https://doi.org/10.33472/AFJBS.6.6.2024.118-133
23. Hachim M.S., Rajab J.M., Al-Salihi, A.M., and Lim, H.S. (2024b). Spatiotemporal Variability and Trend of Ozone Pollution from Satellite data (2003-2021) in Iraq, *Iraqi Journal of Science,* ***65***(10SI), 5909-5920. https://doi.org/10.24996/ijs.2024.65.10(SI).2
24. Han HS, Seok J, and Park KY. (2025). Air Pollution and Skin Diseases, *Ann Dermatology,* ***37***(2):53-67. https://doi.org/10.5021/ad.24.159. PMID: 40165563; PMCID: PMC11965873.
25. Han, S., Bian, H., Feng, Y., Liu, A., and Zhang, X. (2011). Analysis of the relationship between O_3, NO, and NO_2 in Tianjin, China, *Aerosol and Air Quality Research,* ***11***(2), 128–139. https://doi.org/10.4209/aaqr.2010.07.0055
26. Hashim, B.M., Al-Naseri, S.K., Al-Maliki, A., and Al-Ansari, N. (2021). Impact of COVID-19 lockdown on NO_2, O_3, $PM_{2.5}$ and PM_{10} concentrations and assessing air quality changes in Baghdad, Iraq, *Science of the Total Environment,* ***746***, 141978. https://doi.org/10.1016/j.scitotenv.2020.141221

ACCEPTED MANUSCRIPT

27. He, J., Gong, S., Yu, Y., Yu, L., Wu, L., Mao, H., Song, C., Zhao, S., Liu, H., Li, X., and Li, R. (2017). Air pollution characteristics and their relation to meteorological conditions during 2014–2015 in major Chinese cities, *Environmental Pollution,* ***223***, 484-496. https://:doi.org/10.1016/j.envpol. 2017.01.050
28. Hoffmann, B., Boogaard, H., de Nazelle, A., Andersen, Z.J., Abramson, M., Brauer, M., *et al.* (2021). WHO Air Quality Guidelines 2021–Aiming for Healthier Air for all: A Joint Statement by Medical, Public Health, Scientific Societies and Patient Representative Organizations. *International Journal of Public Health,* ***66***. https://doi.org/10.3389/ijph.2021.1604465
29. Huangfu, P., and Atkinson, R. (2020). Long-term exposure to NO_2 and O_3 and all-cause and respiratory mortality: A systematic review and meta-analysis, *Environment International,* ***144***, 105998. https://doi.org/10.1016/ j.envint.2020.105998
30. Ilić, P., Popović, Z., and Markić, D.N. (2020). Assessment of Meteorological Effects and Ozone Variation in Urban Area, *Ecological Chemistry and Engineering Society*, ***27***(3), 373–385. https://doi.org/10.2478/eces-2020-0024
31. Iraq-Wikipedia. (n.d.). Retrieved July 14, 2025, from https://en.wikipedia.org/ wiki/Iraq
32. Jassim, S.Z. and Goff, J.C. (2006) *Geology of Iraq*. 1st Edition, published by Dolin, Prague and Moravian Museum, Brno, Printed in the Czech Republic. ISBN 80-7028-287-8.
33. Jones, A.M., Harrison, R.M., and Baker, J. (2010). The wind speed dependence of the concentrations of airborne particulate matter and NO_x, *Atmospheric Environment,* ***44***(13), 1682–1690. https://doi.org/https://doi.org/10.1016/j. atmosenv.2010.01.007
34. Klein, P.M., Hu, XM. and Xue, M. (2014). Impacts of Mixing Processes in Nocturnal Atmospheric Boundary Layer on Urban Ozone Concentrations, *Boundary-Layer Meteorology* ***150***, 107–130. https://doi.org/10.1007/s10546-013-9864-4
35. Kobza, J., Dul, L., and Geremek, M. (2024). The influence of NOx, temperature, wind and total radiation on the level of ozone concentration in the Upper Silesian agglomeration, *Frontiers in Public Health,* ***12,*** 1485333. https://doi.org/10.3389/fpubh.2024.1485333
36. Lelieveld, J., Beirle, S., Hörmann, C., Stenchikov, G., and Wagner, T. (2015). Abrupt recent trend changes in atmospheric nitrogen dioxide over the Middle East, *Science Advances, 1*(7). https://doi.org/10.1126/sciadv.1500498
37. Li, J., Carlson, B.E., Yung, Y.L., Lv, D., Hansen, J., Penner, J.E., *et al.* (2022). Scattering and absorbing aerosols in the climate system, *Nature Reviews Earth & Environment,* ***3***(6), 363–379. https://doi.org/10.1038/s43017-022-00296-7
38. Ministry of Planning, R. of I. (n.d.). *Central Statistical Organization* – Republic of Iraq, Ministry of Planning. Https://Mop.Gov.Iq/En/Central-Statistical-Organization.

ACCEPTED MANUSCRIPT

39. Mohammed, Z.B., Kamal, A.A.K., Resheq, A.S., and Alabdraba, W.M.Sh. (2019). Assessment of Air Pollution over Baghdad City Using Fixed Annual Stations and GIS Techniques, *Journal of Southwest Jiaotong University,* ***54***(6). https://doi.org/10.35741/issn.0258-2724.54.6.36
40. Nguyen, D-H., Lin, C., Vu, C-T., Cheruiyot, N.K., Nguyen, M.K., Le, T.H., *et al.* (2022). Tropospheric ozone and NOx: A review of worldwide variation and meteorological influences, *Environmental Technology and Innovations,* ***28***, 102809. https://doi.org/10.1016/j.eti.2022.102809
41. Román-Cascón, C., Yagüe, C., Ortiz-Corral, P., Serrano, E., Sánchez, B., Sastre, M., *et al.* (2023). Wind and turbulence relationship with NO_2 in an urban environment: a fine-scale observational analysis, *Urban Climate,* ***51***, 101663. https://doi.org/10.1016/j.uclim.2023.101663
42. Salman, A.D., and Hassan, A.S. (2026). Assessing the effect of aerosol optical depth on solar radiation components over Iraq (2010–2022), *Journal of Geography, Environment and Earth Science International,* ***30***(3), 35-51. https://doi.org/10.9734/jgeesi/2026/ v30i31026
43. Schäfer, K., Wagner, P., Emeis, S., Jahn, C., Muenkel, C., Suppan, P. (2012). Mixing layer height and air pollution levels in urban area. *Proceedings of SPIE digital library, 25th Oct 2012*, 8534. https://doi.org/10.1117/12.974328
44. Seinfeld, J.H., and Pandis, S.N. (2016). *Atmospheric chemistry and physics: from air pollution to climate change*. 3rd ed. John Wiley & Sons. ISBN: 978-1-118-94740-1, 1152 pages. https://doi.org/10.1002/9781119233350
45. Shihab A.S., and Al-Jarrah O.A.I. (2015). The levels of ozone and nitrogen oxides and its relationship with metrological factors, *Al-Rafidain Engineering Journal,* ***23***(4), 98-109. [In Arabic]
46. Shihab, A.S. (2022). Identification of Air Pollution Sources and Temporal Assessment of Air Quality at a Sector in Mosul City Using Principal Component Analysis, *Polish Journal of Environmental Studies, 31*(3), 2223–2235. https://doi.org/10.15244/pjoes/143295
47. Sillman, S. (1999). The relation between ozone, NOx and hydrocarbons in urban and polluted rural environment, *Atmospheric Environment,* ***33***(12), 1821-1845. https://doi.org/10.1016/S1352-2310(98)00345-8
48. Smoydzin, L., Fnais, M., and Lelieveld, J. (2012). Ozone pollution over the Arabian Gulf – role of meteorological conditions, *Atmospheric Chemistry and Physics Discussions,* ***12***(2), 6331–6366. https://doi.org/10.519 4/acpd-12-6331-2012
49. Stohl, A., Forster, C., Eckhardt, S., Spichtinger, N., Huntrieser, H., Heland, J., *et al.* (2003). A backward modeling study of intercontinental pollution transport using aircraft measurements.

ACCEPTED MANUSCRIPT

Journal of Geophysical Research: Atmospheres, ***108***(D12), 4370. https://doi.org/10.1029/2002JD002862

50. Tang, G., Li, X., Wang, Y., Xin, J., and Ren, X. (2009). Surface ozone trend details and interpretations in Beijing, 2001–2006, *Atmospheric Chemistry and Physics,* ***9***(22), 8813–8823. https://:doi.org/10.5194/acp-9-8813-2009
51. Tao, Y., Huang, W., Xiang, X., Zhong, L., Lu, S.E., Li, Y., *et al.* (2012). Estimated acute effects of ambient ozone and nitrogen dioxide on mortality in the Pearl River Delta of southern China, *Environmental Health Perspectives,* ***120***(3), 393–398. https://doi.org/10.1289/ehp.1115720
52. Vardoulakis, S., Fisher, B.E., Pericleous, K., and Gonzalez-Flesca, N. (2003). Modelling air quality in street canyons: a review, *Atmospheric Environment,* ***37***(2), 155-182. https://doi.org/10.1016/S1352-2310(02)00857-9
53. Wang, Y., Cai, L., Shi, G.Y., Liu, C.G., Yao, L.J., Li, H., *et al.* (2026). From traffic flow to ozone surges: Exploring threshold effects and interactive drivers of urban ozone pollution in arid regions, *Urban Climate,* ***65***, 102801. https://doi.org/10.1016/j.uclim.2026.102801
54. Wang, Y., Yang, Y., Yuan, Q., Li, T., Zhou, Y., Zong, L., *et al.* (2025). Substantially underestimated global health risks of current ozone pollution, *Nature Communications, 16*, 102. https://doi.org/10.1038/s41467-024-55450-0
55. WHO (2022). *Ambient (outdoor) air pollution-WHO*. https://iris.who.int/server/api/core/bitstreams/551b515e-2a32-4e1a-a58c-cdaecd395b19/content
56. Xia, X., Meng, X., Liu, C., Guo, Y., Li, X., Niu, Y., *et al.* (2024). Associations of long-term nitrogen dioxide exposure with a wide spectrum of diseases: a prospective cohort study of 0·5 million Chinese adults, *The Lancet Public Health,* ***9***(12), e1047-e1058. https://doi.org/10.1016/S2468-2667(24)00264-0
57. Yang, Z., Du, Q., Yang, Q., Zhao, C., Li, G., Xia, Z., *et al.* (2025) Modeling urban pollutant transport at multiple resolutions: impacts of turbulent mixing, *Atmospheric Chemistry and Physics,* ***25***, 8831–8857. https://doi.org/10.5194/acp-25-8831-2025
58. Yildizhan, H., Udriștioiu, M. T., Pekdogan, T., and Ameen, A. (2024). Observational study of ground-level ozone and climatic factors in Craiova, Romania, based on one-year high-resolution data, *Scientific Reports,* ***14***(1), 26733. https://doi.org/10.1038/s41598-024-77989-0
59. Yin, P., Chen, R., Wang, L., Meng, X., Liu, C., Niu, Y., *et al.* (2017). Short-term effects of ambient ozone on mortality in 31 Chinese capital cities, *Environmental Health Perspectives,* ***125***(4), 047011. https://doi.org/10.1289/EHP184
60. Zakaria, S., Al-Ansari, N., and Knutsson, S. (2013). Historical and Future Climatic Scenarios for Temperature and Rainfall in Iraq, *Journal of Civil Engineering and Architecture,* ***7***(12), 1584-1594. https://doi.org/10.17265/19347359/2013.12.012

ACCEPTED MANUSCRIPT

61. Zhang, T., Xu, X., and Su., Y. (2020). Impacts of Regional Transport and Meteorology on Ground-Level Ozone in Windsor, Canada, *Atmosphere,* ***11***(10): 1111. https://doi.org/10.3390/atmos11101111
62. Zhao, S., Yu, Y., and Li, J. (2020). Effects of precipitation on air pollution in spring and summer in Lanzhou, *E3S Web of Conferences,* ***194***:04007. https://doi.org/10.1051/e3sconf/202019404007

ACCEPTED MANUSCRIPT